

# L2 OSTC-CPM: Theory and design

Matthias Hesse\*, Jérôme Lebrun and Luc Deneire

Lab. I3S, CNRS, University of Nice, Sophia Antipolis, France

E-Mail: {hesse, lebrun, deneire}@i3s.unice.fr

The combination of space-time coding (STC) and continuous phase modulation (CPM) is an attractive field of research because both STC and CPM bring many advantages for wireless communications. Zhang and Fitz [1] were the first to apply this idea by constructing a trellis based scheme. But for these codes the decoding effort grows exponentially with the number of transmitting antennas. This was circumvented by orthogonal codes introduced by Wang and Xia [2]. Unfortunately, based on Alamouti code [3], this design is restricted to two antennas.

However, by relaxing the orthogonality condition, we prove here that it is possible to design  $L^2$ -orthogonal space-time codes which achieve full rate and full diversity with low decoding effort. In part one, we generalize the two-antenna code proposed by Wang and Xia [2] from pointwise to  $L^2$ -orthogonality and in part two we present the first  $L^2$ -orthogonal code for CPM with three antennas. In this report, we detail these results and focus on the properties of these codes. Of special interest is the optimization of the bit error rate which depends on the initial phase of the system. Our simulation results illustrate the systemic behavior of these conditions.

## 1 Part one: Two antennas case

To combine the high power efficiency of Continuous Phase Modulation (CPM) with either high spectral efficiency or enhanced performance in low Signal to Noise conditions, some authors have proposed to introduce CPM in a MIMO frame, by using Space Time Codes (STC). In this part, we address the code design problem of Space Time Block Codes combined with CPM and introduce a new design criterion based on  $L^2$  orthogonality. This  $L^2$  orthogonality condition, with the help of simplifying assumption, leads, in the 2x2 case, to a new family of codes. These codes generalize the Wang and Xia code, which was based on pointwise orthogonality. Simulations indicate that the new codes achieve full diversity and a slightly better coding gain. Moreover, one of the codes can be interpreted as two antennas fed by two conventional CPMs using the same data but with different alphabet sets. Inspection of these alphabet sets lead also to a simple explanation of the (small) spectrum broadening of Space Time Coded CPM.

### 1.1 Introduction

Since the pioneer work of Alamouti [3] and Tarokh [4], Space Time Coding has been a fast growing field of research where numerous coding schemes have been introduced. Several years later Zhang and Fitz [1, 5] were the first to apply the idea of STC to continuous phase modulation (CPM) by constructing trellis codes. In [6] Zajić and Stüber derived conditions for partial response STC-CPM to get full diversity and optimal coding gain. A STC for noncoherent detection based on diagonal blocks was introduced by Silvester et al. [7].

The first orthogonal STC for CPM for full and partial response was developed by Wang and Xia [8, 2]. The scope of this part is also the design of an orthogonal STC for CPM. But unlike Wang-Xia approach [2] which starts from a QAM orthogonal Space-Time Code (e.g. Alamouti's scheme [3]) and modify it to achieve continuous phases for the transmitted signals, we show here that a more general  $L^2$  condition is sufficient to ensure fast maximum likelihood decoding with full diversity.

In the considered system model (Fig. 1), the data sequence  $d_j$  is defined over the signal constellation set

$$\Omega_d = \{-M + 1, -M + 3, \dots, M - 3, M - 1\} \quad (1)$$

for an alphabet with  $\log_2 M$  bits. To obtain the structure for a Space Time Block Code (STBC) this sequence is mapped to data matrices  $\mathbf{D}^{(i)}$  with elements  $d_{mr}^{(i)}$ , where  $m$  denotes the transmitting antenna,  $r$  the time slot into a block and  $(i)$  a parameter for partial response CPM. The data matrices are then used to modulate the sending matrix

$$\mathbf{S}(t) = \begin{bmatrix} s_{11}(t) & s_{12}(t) \\ s_{21}(t) & s_{22}(t) \end{bmatrix}. \quad (2)$$

---

\*The work of Matthias Hesse is supported by a EU Marie-Curie Fellowship (EST-SIGNAL program : <http://est-signal.i3s.unice.fr>) under contract No MEST-CT-2005-021175.

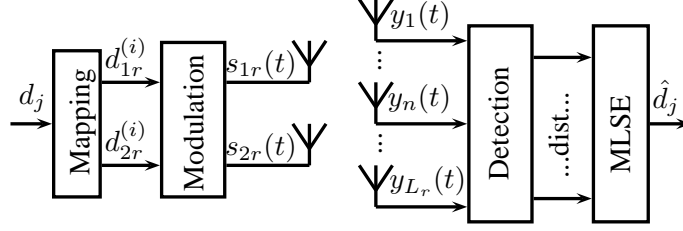


Figure 1: Structure of a MIMO Tx/Rx system

Each element is defined for  $(2l + r - 1)T \leq t \leq (2l + r)T$  as

$$s_{mr}(t) = \sqrt{\frac{E_s}{T}} e^{j2\pi\phi_{mr}(t)} \quad (3)$$

where  $E_s$  is the symbol energy and  $T$  the symbol time. The phase  $\phi_{mr}(t)$  is defined in the conventional CPM manner [9] with an additional correction factor  $c_{mr}(t)$  and is therewith given by

$$\phi_{mr}(t) = \theta_m(2l + r) + h \sum_{i=2l+1+r-\gamma}^{2l+r} d_{mr}^{(i)} q(t - (i - 1)T) + c_{mr}(t) \quad (4)$$

where  $h = 2m_0/p$  with  $m_0$  and  $p$  relative primes is called the modulation index. The phase smoothing function  $q(t)$  has to be a continuous function with  $q(t) = 0$  for  $t \leq 0$  and  $q(t) = 1/2$  for  $t \geq \gamma T$ .

The memory length  $\gamma$  determines the length of  $q(t)$  and affects the spectral compactness. For large  $\gamma$  we obtain a compact spectrum but also a higher number of possible phase states which increases the decoding effort. For full response CPM, we have  $\gamma = 1$  and for partial response systems  $\gamma > 1$ .

The choice of the correction factor  $c_{mr}(t)$  in Eq. (4) is along with the mapping of  $d_j$  to  $\mathbf{D}^{(i)}$ , the key element in the design of our coding scheme. It will be detailed in Section 1.2. We then define  $\theta_m(2l + r)$  in a most general way

$$\theta_m(2l + 3) = \theta_m(2l + 2) + \xi(2l + 2) = \theta_m(2l + 1) + \xi(2l + 1) + \xi(2l + 2). \quad (5)$$

The function  $\xi(2l + r)$  will be fully defined from the contribution  $c_{mr}(t)$  to the phase memory  $\theta_m(2l + r)$ . For conventional CPM system,  $c_{mr}(t) = 0$  and we have  $\xi(2l + 1) = \frac{h}{2} d_{2l+1-\gamma}$ .

The channel coefficients  $\alpha_{mn}$  are assumed to be Rayleigh distributed and independent. Each coefficient  $\alpha_{mn}$  characterizes the fading between the  $m^{\text{th}}$  transmit (Tx) antenna and the  $n^{\text{th}}$  receive (Rx) antenna where  $n = 1, 2, \dots, L_r$ . Furthermore, the received signals

$$y_n(t) = \alpha_{mn} s_{mr}(t) + n(t) \quad (6)$$

are corrupted by a complex additive white Gaussian noise  $n(t)$  with variance  $1/2$  per dimension.

At the receiver, the detection is done on each of the  $L_r$  received signals separately. Therefore, in general, each code block  $\mathbf{S}(t)$  has to be detected by block. E.g. for a 2x2 block, estimating the symbols  $\hat{d}_j$  implies computational complexity proportional to  $M^2$ . Now, this complexity can be reduced to  $2M$  by introducing an orthogonality property as well as simplifying assumptions on the code.

Criteria for such STBC are given in Section 1.2. In Section 1.3, the criteria are used to construct OSTBC for CPM. In Section 1.4 we test the designed code and compare it with the STC from Wang and Xia [2]. Finally, some conclusions are drawn in Section 1.5.

## 1.2 Design Criteria

The purpose of the design is to achieve full diversity and a fast maximum likelihood decoding while maintaining the continuity of the signal phases. This section shows how the need to perform fast ML decoding leads to the  $L^2$  orthogonality condition as well as to simplifying assumptions, which can be combined with the continuity conditions. For convenience we only consider one Rx antenna and drop the index  $n$  in  $\alpha_{mn}$ .

### 1.2.1 Fast Maximum Likelihood Decoding

Commonly, due to the trellis structure of CPM, the Viterbi algorithm is used to perform the ML demodulation. On block  $l$  each state in the trellis has  $M^2$  incoming branches and  $M^2$  outgoing branches with a distance

$$D_l = \int_{2lT}^{(2l+1)T} \left| y(t) - \sum_{m=1}^2 \alpha_m s_{m1}(t) \right|^2 dt + \int_{(2l+1)T}^{(2l+2)T} \left| y(t) - \sum_{m=1}^2 \alpha_m s_{m2}(t) \right|^2 dt. \quad (7)$$

The number of branches results from the blockwise decoding and the correlation between the sent symbols  $s_{1r}(t)$  and  $s_{2r}(t)$ . A way to reduce the number of branches is to structurally decorrelate the signals sent by the two transmitting antennas, i.e. to put to zero the inter-antenna correlation

$$\alpha_2 \alpha_1^* \int_{2lT}^{(2l+1)T} s_{21}(t) s_{11}^*(t) dt + \alpha_1 \alpha_2^* \int_{2lT}^{(2l+1)T} s_{11}(t) s_{21}^*(t) dt + \alpha_2 \alpha_1^* \int_{(2l+1)T}^{(2l+2)T} s_{22}(t) s_{12}^*(t) dt + \alpha_1 \alpha_2^* \int_{(2l+1)T}^{(2l+2)T} s_{12}(t) s_{22}^*(t) dt = 0. \quad (8)$$

Pointwise orthogonality as defined in [2] is therefore a sufficient condition but not necessary. A less restrictive  $L^2$  orthogonality is also sufficient. From Eq. (8), the distance given in Eq. (7) can then be simplified to

$$D_l = \int_{2lT}^{(2l+1)T} f_{11}(t) + f_{21}(t) - |y(t)|^2 dt + \int_{(2l+1)T}^{(2l+2)T} f_{12}(t) + f_{22}(t) - |y(t)|^2 dt \quad (9)$$

with  $f_{mr}(t) = |y(t) - \alpha_m s_{mr}(t)|^2$ . When each  $s_{mr}(t)$  depends only on  $d_{2l+1}$  or  $d_{2l+2}$  the branches can be split and calculated separately for  $d_{2l+1}$  and  $d_{2l+2}$ . The complexity of the ML decision is reduced to  $2M$ . The complexity for detecting two symbols is thus reduced from  $pM^{\gamma+1}$  to  $pM^\gamma$ . The STC introduced by Wang and Xia [2] didn't take full advantage of the orthogonal design since  $s_{mr}(t)$  was depending on both  $d_{2l+1}$  and  $d_{2l+2}$ . The gain they obtained in [2] was then relying on other properties of CPM, e.g. some restrictions put on  $q(t)$  and  $p$ . These restrictions may also be applied to our design code, which would lead to additional complexity reduction.

### 1.2.2 Orthogonality Condition

In this section we show how  $L^2$  orthogonality for CPM, i.e.  $\|\mathbf{S}(t)\|_{L^2}^2 = \int_{2lT}^{(2l+2)T} \mathbf{S}(t) \mathbf{S}^H(t) dt = 2\mathbf{I}$ , can be obtained. As such, the correlation between the two transmitting antennas per coding block is canceled if

$$\int_{2lT}^{(2l+2)T} s_{1r}(t) s_{2r}^*(t) dt = \int_{2lT}^{(2l+1)T} s_{11}(t) s_{21}^*(t) dt + \int_{(2l+1)T}^{(2l+2)T} s_{12}(t) s_{22}^*(t) dt = 0. \quad (10)$$

Replacing  $s_{mr}(t)$  by the corresponding CPM symbols from Eq. (4), we get

$$\begin{aligned} & \int_{2lT}^{(2l+1)T} \exp \left\{ j2\pi \left[ \theta_1(2l+1) + h \sum_{i=2l+2-\gamma}^{2l+1} d_{1,1}^{(i)} q(t - (i-1)T) + c_{1,1}(t) - \theta_2(2l+1) - h \sum_{i=2l+3-\gamma}^{2l+2} d_{2,1}^{(i)} q(t - (i-1)T) - c_{2,1}(t) \right] \right\} dt + \\ & \int_{(2l+1)T}^{(2l+2)T} \exp \left\{ j2\pi \left[ \theta_1(2l+2) + h \sum_{i=2l+3-\gamma}^{2l+2} d_{1,2}^{(i)} q(t - (i-1)T) + c_{1,2}(t) - \theta_2(2l+2) - h \sum_{i=2l+2-\gamma}^{2l+1} d_{2,2}^{(i+1)} q(t - iT) - c_{2,2}(t) \right] \right\} dt = 0. \end{aligned} \quad (11)$$

The phase memory  $\theta_m(2l+r)$  is independent of time and has not to be considered for integration. Using Eq. (5) to replace phase memory  $\theta_m(2l+2)$  of the second time slot, we obtain

$$\begin{aligned} & \int_{2lT}^{(2l+1)T} \exp \left\{ j2\pi \left[ h \sum_{i=2l+2-\gamma}^{2l+1} d_{1,1}^{(i)} q(t - (i-1)T) + c_{1,1}(t) - h \sum_{i=2l+2-\gamma}^{2l+1} d_{2,1}^{(i)} q(t - (i-1)T) - c_{2,1}(t) \right] \right\} dt + \exp \left\{ j2\pi [\xi_1(2l+1) - \xi_2(2l+1)] \right\} \cdot \\ & \int_{2lT}^{(2l+1)T} \exp \left\{ j2\pi \left[ h \sum_{i=2l+2-\gamma}^{2l+1} d_{1,2}^{(i+1)} q(t - (i-1)T) + c_{1,2}(t+T) - h \sum_{i=2l+2-\gamma}^{2l+1} d_{2,2}^{(i+1)} q(t - (i-1)T) - c_{2,2}(t+T) \right] \right\} dt = 0. \end{aligned} \quad (12)$$

### 1.2.3 Simplifying assumptions

To simplify this expression, we factor Eq. (12) into a time independent and a time dependent part. For merging the two integrals to one time dependent part, we have to map  $d_{m2}^{(i)}$  to  $d_{m1}^{(i)}$  and  $c_{mr}(t)$  to a different  $c_{m'r'}(t)$ . Consequently, for the data symbols  $d_{mr}^{(i)}$  there exist three possible ways of mapping:

- *crosswise mapping* with  $d_{1,1}^{(i)} = d_{2,2}^{(i)}$  and  $d_{1,2}^{(i)} = d_{2,1}^{(i)}$ ;
- *repetitive mapping* with  $d_{1,1}^{(i)} = d_{1,2}^{(i)}$  and  $d_{2,1}^{(i)} = d_{2,2}^{(i)}$ ;
- *parallel mapping* with  $d_{1,1}^{(i)} = d_{2,1}^{(i)}$  and  $d_{1,2}^{(i)} = d_{2,2}^{(i)}$ .

The same approach can be applied to  $c_{mr}(t)$ :

- *crosswise mapping* with  $c_{11}(t) = -c_{22}(t - T)$  and  $c_{12}(t) = -c_{21}(t - T)$ ;
- *repetitive mapping* with  $c_{11}(t) = c_{12}(t - T)$  and  $c_{21}(t) = c_{22}(t - T)$ ;
- *parallel mapping* with  $c_{11}(t) = c_{21}(t)$  and  $c_{12}(t) = c_{22}(t)$ .

For each combination of mappings, Eq. (12) is now the product of two factors, one containing the integral and the other a time independent part. To fulfill Eq. (12) it is sufficient if one factor is zero, namely  $1 + e^{j2\pi[\xi_1(2l+1) - \xi_2(2l+1)]} = 0$ , i.e. if

$$k + \frac{1}{2} = \xi_1(2l+1) - \xi_2(2l+1) \quad (13)$$

with  $k \in \mathbb{N}$ . We thus get a very simple condition which only depends on  $\xi_m(2l+1)$ .

### 1.2.4 Continuity of Phase

In this section we determine the functions  $\xi_m(2l+1)$  to ensure the phase continuity.

Precisely, the phase of the CPM symbols has to be equal at all intersections of symbols. For an arbitrary block  $l$ , it means that  $\phi_{m1}((2l+1)T) = \phi_{m2}((2l+1)T)$ . Using Eq. (4), it results in

$$\xi_m(2l+1) = h \sum_{i=2l+2-\gamma}^{2l+1} d_{m,1}^{(i)} q((2l+2-i)T) + c_{m,1}((2l+1)T) - h \sum_{i=2l+3-\gamma}^{2l+2} d_{m,2}^{(i)} q((2l+2-i)T) - c_{m,2}((2l+1)T). \quad (14)$$

For the second intersection at  $(2l+2)T$ , since  $\phi_{m2}((2l+2)T) = \phi_{m1}((2l+2)T)$ , we get

$$\xi_m(2l+2) = h \sum_{i=2l+3-\gamma}^{2l+2} d_{m,1}^{(i)} q((2l+3-i)T) + c_{m,1}((2l+2)T) - h \sum_{i=2(l+1)+2-\gamma}^{2(l+1)+1} d_{m,2}^{(i)} q((2l+3-i)T) - c_{m,2}((2l+2)T). \quad (15)$$

Now, by choosing one of the mappings detailed in Section 1.3, these equations can be greatly simplified. Hence, we have all the tools to construct our code.

## 1.3 Orthogonal Space Time Codes

In this section we will have a closer look at two codes constructed under the afore-mentioned conditions.

### 1.3.1 Existing Code

As a first example, we will give an alternative construction of the code given by Wang and Xia in [2]. Indeed, the pointwise orthogonality condition used by Wang and Xia is a special case of the  $L^2$  orthogonality condition, hence, their ST-code can be obtained within our framework.

For the first antenna Wang and Xia use a conventional CPM with  $d_{1r}^{(i)} = d_i$  for  $i = 2l+r+1-\gamma, 2l+r+2-\gamma, \dots, 2l+r$  and  $c_{1r}(t) = 0$ . The symbols of the second antenna are mapped *crosswise* to the first  $d_{21}^{(i)} = -d_{i+1}$  for  $i = 2l+2-\gamma, 2l+3-\gamma, \dots, 2l+1$  and  $d_{22}^{(i-1)} = -d_{i-1}$  for  $i = 2l+3-\gamma, 2l+4-\gamma, \dots, 2l+2$ . Using this cross mapping makes it difficult to compute  $\xi_m(2l+1)$  since the CPM typical order of the data symbols is mixed. Wang and Xia circumvent this by introducing another correction factor for the second antenna

$$c_{2r}(t) = \sum_{i=0}^{\gamma-1} (h(d_{2l+1-i} + d_{2l+2-i}) + 1) q_0(t - (2l+r-1-i)T). \quad (16)$$

By first computing  $\xi_m(2l+1)$  with Eq. (17) and then Eq. (13), we get the  $L^2$  orthogonality of the Wang-Xia-STC.

### 1.3.2 Parallel Code

To get a simpler correction factor as in [2], we designed a new code based on the *parallel* structure which permits to maintain the conventional CPM mapping for both antennas. Hence we choose the following mapping:  $d_{m1}^{(i)} = d_{m2}^{(i-1)} = d_i$  for  $i = 2l+r+1-\gamma, 2l+r+2-\gamma, \dots, 2l+r$ . Then, Eq. (14) and (15) can be simplified into

$$\xi_m(2l+1) = \frac{h}{2} d_{2l+2-\gamma} + c_{m1}((2l+1)T) - c_{m2}((2l+1)T) \quad \xi_m(2l+2) = \frac{h}{2} d_{2l+3-\gamma} + c_{m2}((2l+2)T) - c_{m1}((2l+2)T). \quad (17)$$

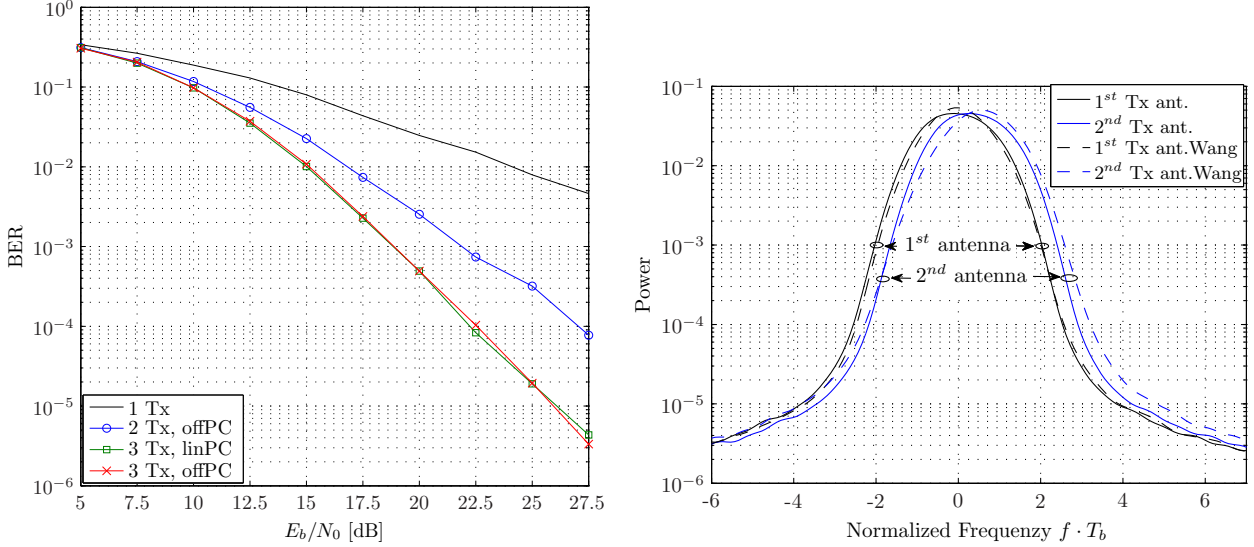


Figure 2: Left: Simulated BER for different numbers of Tx and Rx antennas of the proposed STC and of the Wang-Xia-STC; Right: Simulated psd for each Tx antenna of the proposed STC (continuous line) and the Wang-Xia-STC (dashed line)

With this simplified functions, the orthogonality condition only depends on the start and end values of  $c_{mr}(t)$ , i.e.

$$k + \frac{1}{2} = c_{11}((2l+1)T) - c_{12}((2l+1)T) - c_{21}((2l+1)T) + c_{22}((2l+1)T). \quad (18)$$

To merge the two integrals in Eq. (12), the mapping of  $d_{mr}^{(i)}$  is necessary but also an equality between different  $c_{mr}(t)$ . From the three possible mappings, we choose the *repeat mapping* because of the possibility to set  $c_{mr}(t)$  to zero for one antenna. Hence we are able to send a conventional CPM signal on one antenna and a modified one on the second. Using Eq. (18) and the equalities for the mapping, we can formulate the following condition

$$k + \frac{1}{2} = c_{12}(2lT) - c_{12}((2l+1)T) - c_{22}(2lT) + c_{22}((2l+1)T). \quad (19)$$

With  $c_{11}(t) = c_{12}(t) = 0$ , we can take for  $c_{21}(t) = c_{22}(t)$  any continuous function which is zero at  $t = 0$  and  $1/2$  at  $t = T$ . Another possibility is to choose the correction factor of the second antenna with a structure similar to CPM modulation, i.e.

$$c_{2r}(t) = \sum_{i=2l+1-\gamma}^{2l+1} q(t - (i-1)T) \quad (20)$$

for  $(2l+r-1)T \leq t \leq (2l+r)T$ . With this approach, the correction factors can be included in a classical CPM modulation with constant offset of  $1/h$ . This offset may also be expressed as a modified alphabet for the second antenna

$$\Omega_{d_2} = \left\{ -M + 1 + \frac{1}{h}, -M + 3 + \frac{1}{h}, \dots, M - 3 + \frac{1}{h}, M - 1 + \frac{1}{h} \right\}. \quad (21)$$

Consequently, this  $L^2$ -orthogonal design may be seen as two conventional CPM designs with different alphabet sets  $\Omega_d$  and  $\Omega_{d_2}$  for each antenna. However, in this method, the constant offset to the phase may cause a shift in frequency. But as shown by our simulations in the next section, this shift is quite moderate.

## 1.4 Simulations

In this section we verify the proposed algorithm by simulations. Therefore a STC-2REC-CPM-sender with two transmitting antennas has been implemented in MATLAB. For the signal of the first antenna we use conventional Gray-coded CPM with a modulation index  $h = 1/2$ , the length of the phase response function  $\gamma = 2$  and an alphabet size of  $M = 8$ . The signal of the second antenna is modulated by a CPM with the same parameters but a different alphabet  $\Omega_{d_2}$ , corresponding to Eq. (21).

The channel used is a frequency flat Rayleigh fading model with additive white Gaussian noise. The fading coefficients  $\alpha_{mn}$  are constant for the duration of a code block (block fading) and known at receiver (coherent detection). The received signal  $y_n(t)$  is demodulated by two filterbanks with  $pM^2$  filters, which are used to calculate the correlation between the received and candidate signals. Due to the orthogonality of the antennas each filterbank is independently

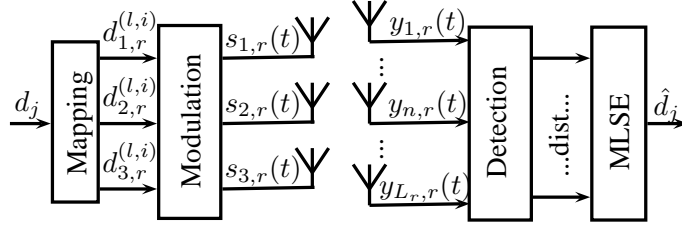


Figure 3: Structure of a MIMO Tx/Rx system

applied to the corresponding time slot  $k$  of the block code. The correlation is used as metric for the Viterbi algorithm (VA) which has  $pM$  states and  $M$  paths leaving each state. In our simulation, the VA is truncated to a path memory of 10 code blocks, which means that we get a decoding delay of  $2 \cdot 10T$ .

From the simulation results given in Figure 2, we can reasonably assume that the proposed code achieves full diversity. Indeed, the curves for the 2x1 and 2x2 systems respectively show a slope of 2 and 4. Moreover, the curve of the 2x1 systems follows the same slope as the ST code proposed by Wang and Xia [2], which was proved to have full diversity. Note also that the new code provides a slightly better performance.

A main reason of using CPM for STC is the spectral efficiency. Figure 2 show the simulated power spectral density (psd) for both Tx antennas of the proposed ST code (continuous line) and the ST code proposed by Wang and Xia [2]. The first antenna of our approach uses a conventional CPM signal and hence shows an equal psd. The spectrum of the second antenna is shifted due to adding an offset  $c_{mr}(t)$  with a non zero mean. Minimizing the difference between the two spectra by shifting one, result in a phase difference of 0.375 measured in normalized frequency  $f \cdot T_d$ , where  $T_d = T/\log_2(M)$  is the bit symbol length. The first antenna of the Wang-Xia-algorithm has almost the same psd while the spectrum of the second antenna is shifted by approximately  $0.56f \cdot T_d$ . This means that the OSTC by Wang and Xia requires a slightly larger bandwidth than our OSTC.

## 1.5 Conclusion to part one

In applications where the power efficiency is crucial, combination of Continuous Phase Modulation and Space Time Coding has the potential to provide high spectral efficiency, thanks to spatial diversity. To address this power efficiency, ST code design for CPM has to ensure both low complexity decoding and full diversity. To fulfill these requirements, we have proposed a new  $L^2$  orthogonality condition. We have shown that this condition is sufficient to achieve low complexity ML decoding and leads, with the help of simplifying assumption to a simple code. Moreover, simulations indicate that the code most probably achieves full diversity. In the next part of this report, we will concentrate on the design of other codes based on  $L^2$  orthogonality and will show how to design full diversity, full rate  $L^2$  orthogonal codes for 3 antennas.

## 2 Part two: Extension to more antennas

To combine the power efficiency of Continuous Phase Modulation (CPM) with enhanced performance in fading environments, some authors have suggested to use CPM in combination with Space-Time Codes (STC). In part one, we have proposed a CPM ST-coding scheme bases on  $L^2$ -orthogonality for two transmitting antennas. In this part we extend this approach to the three antenna case. We analytically derive a family of coding schemes which we call Parallel Code (PC). This code family has full rate and we expect that the proposed coding scheme achieves full diversity. This is confirmed by accompanying simulations. We detail an example for the proposed STC which can be interpreted as a conventional CPM scheme with different alphabet sets for the different transmit antennas which results in simplified implementation. Thanks to  $L^2$ -orthogonality, the decoding complexity, usually exponentially proportional to the number of transmitting antennas, is reduced to linear complexity.

### 2.1 Introduction

To overcome the reduction of channel capacity caused by fading, Telatar [10], Foschini and Gans [11] described in the late 90s the potential gain of switching to multiple input multiple output (MIMO) systems. These results triggered many advances mostly concentrated on the coding aspects for transmitting antennas, e.g. Alamouti [3] and Tarokh et al. [4] for Space-Time Block Codes (STBC) and also Tarokh et al. [12] for Space-Time Trellis Codes.

Zhang and Fitz [1, 5] were the first to apply the idea of STC to CPM by constructing trellis codes. In [7], Silvester et al. derived a diagonal block space-time code which enables non-coherent detection. A condition for optimal coding gain while sustaining full diversity was also recently derived by Zajić and Stüber [6].

Inspired by orthogonal design codes, Wang and Xia introduced in [8] the first orthogonal STC for two transmitting antennas and full response CPM and later in [2] for partial response. Their approach was extended in [13] to construct a pseudo-orthogonal ST-coded CPM for four antennas. To avoid the structural limitation of orthogonal design, we proposed in [14] a STC CPM scheme based on  $L^2$  orthogonality for two antennas. Sufficient conditions for  $L^2$  orthogonality were described,  $L^2$  orthogonal codes were introduced and the simulation results displayed good performance and full rate. Here, motivated by this results, we extend our previous work and generalize these conditions for three transmitting antenna.

The main result of the three transmit antenna case, is that it can, unlike the codes based on orthogonal design, achieve full diversity with a full rate code:

1. **the full rate property** is one of the main advantage of using the  $L^2$  norm criterion, instead of merely extending the classical Tarokh [4] orthogonal design to the CPM case. Indeed, in the classical orthogonal design approach, which is based on optimal decoding for linear modulations, the criterion is expressed as the orthogonality between matrices of elements, each of these elements being a definite integral (usually the output of a matched filter). On the contrary, in the  $L^2$  design approach used for non-linear modulations, the product in Eq. (29) is a definite integral itself, the integrand being the product of two signals. This allows more degrees of freedom and enables the full rate property.
2. **the full diversity property** can be proved in a similar way to the classical case, with the help of the extensions proposed by Zajić and Stüber [6].

Furthermore, it should be pointed out that the proposed coding scheme does not limit any parameter of the CPM. It is applicable to full and partial response CPM as well as to all modulation indexes.

We first give the system model for a multiple input multiple output (MIMO) system with  $L_t$  transmitting (Tx) antennas and  $L_r$  receiving (Rx) antennas (Fig. 3). Later on, we will use this general model to derive a L2-OSTC for CPM for  $L_t = 3$ . The emitted signals  $\mathbf{s}(t)$  are mixed by a channel matrix  $\mathbf{A}$  of dimension  $L_r \times L_t$ . The elements of  $\mathbf{A}$ ,  $\alpha_{n,m}$ , are Rayleigh distributed random variables and characterize the fading between the  $n^{th}$  Rx and the  $m^{th}$  Tx antenna. The Tx signal is disturbed by complex additive white Gaussian noise (AWGN) with variance of 1/2 per dimension which is represented by a  $L_r \times L_t$  matrix  $\mathbf{n}(t)$ . The received signal

$$\mathbf{y}(t) = \mathbf{A}\mathbf{s}(t) + \mathbf{n}(t). \quad (22)$$

has the elements  $y_{n,r}$  and the dimension  $L_r \times L_t$ . We group the transmitted CPM signals into blocks

$$\mathbf{s}(t) = \begin{bmatrix} s_{1,1}(t) & \dots & s_{1,L_t}(t) \\ \vdots & s_{m,r}(t) & \vdots \\ s_{L_t,1}(t) & \dots & s_{L_t,L_t}(t) \end{bmatrix} \quad (23)$$

similar to a ST block code with the difference that now the elements are functions of time and not constant anymore. The elements of Eq. (23) are given by

$$s_{m,r}(t) = \sqrt{\frac{E_s}{L_t T}} \exp(j2\pi\phi_{m,r}(t)) \quad (24)$$

for  $(L_t l + r - 1)T \leq t \leq (L_t l + r)T$  and  $m, r = 1, 2, \dots, L_t$ . Here  $m$  represents the transmitting antenna and  $r$  the relative time slot in the block. The symbol energy  $E_s$  is normalized to the number of Tx antennas  $L_t$  and the symbol length  $T$ . The continuous phase

$$\phi_{m,r}(t) = \theta_m(L_t l + r) + h \sum_{i=1}^{\gamma} d_{m,r}^{(l,i)} q(t - i'T) + c_{m,r}(t) \quad (25)$$

is defined similarly to [9] with an additional correction factor  $c_{m,r}(t)$  detailed in Section 2.2.3. Furthermore,  $l$  is indexing the whole code block,  $i$  the overlapping symbols for partial response and  $i' = L_t l + r - i$ . With this extensive description of the symbol  $d_{m,r}^{(l,i)}$ , we are able to define all possible mapping schemes (cp. Section 2.2.2). The modulation index  $h = 2m_0/p$  is the quotient of two relative prime integers  $m_0$  and  $p$  and the phase smoothing function  $q(t)$  has to be continuous for  $0 \leq t \leq \gamma T$ , 0 for  $t \leq 0$  and  $1/2 \leq \gamma T$ . The memory length  $\gamma$  gives the number of overlapping symbols.

To maintain continuity of phase, we define the phase memory

$$\theta_m(L_t l + r + 1) = \theta_m(L_t l + r) + \xi_m(L_t l + r) \quad (26)$$

in a general way. The function  $\xi(L_t l + r)$  will be fully defined in Section 2.2.3 from the contribution of  $c_{mr}(t)$ . For a conventional CPM system, we have  $c_{mr}(t) = 0$  and  $\xi(2l + 1) = \frac{h}{2}d_{2l+1-\gamma}$ .

In Section 2.2, we derive the  $L^2$  conditions for a CPM with three transmitting antennas and introduce adequate mappings and a family of correction factors. In Section 2.3, we detail some properties of the code. In Section 2.4, we benchmark the code by running some simulations and finally, in Section 2.5, some conclusions are drawn.

## 2.2 Parallel Codes (PC) for 3 antennas

### 2.2.1 $L^2$ Orthogonality

In this section we describe how to enforce  $L^2$  orthogonality on CPM systems with three transmitting antennas. Similarly to [14], we impose  $L^2$  orthogonality by

$$\int_{3lT}^{(3l+3)T} \mathbf{s}(t) \mathbf{s}^H(t) dt = E_S \mathbf{I} \quad (27)$$

where  $\mathbf{I}$  is the  $3 \times 3$  identity matrix. Hence the correlation between two different Tx antennas  $s_{m,r}(t)$  and  $s_{m',r}(t)$  is canceled over a complete STC block if

$$\int_{3lT}^{(3l+3)T} s_{m,r}(t) s_{m',r}^*(t) dt = 0 \quad (28)$$

with  $m \neq m'$ . Now, by using Eq. (24) and (25) we get

$$0 = \sum_{r=1}^3 \int_{(3l+r-1)T}^{(3l+r)T} \exp \left( j2\pi \cdot [\theta_m(3l+r) + h \sum_{i=1}^{\gamma} d_{m,r}^{(l,i)} q(t-i'T) + c_{m,r}(t) - (\theta_{m'}(3l+r) - h \sum_{i=1}^{\gamma} d_{m',r}^{(l,i)} q(t-i'T) - c_{m',r}(t))] \right) dt. \quad (29)$$

The phase memory  $\theta_m(3l+r)$  is time independent and therewith can be moved to a constant factor in front of the integrals. Similarly to [14], we introduce *parallel mapping* ( $d_{m,r}^{(l,i)} = d_{m',r}^{(l,i)}$ ) for the data symbols and *repetitive mapping* ( $c_{m,r}(t) = c_{m',r}(t)$ ) for the correction factors. The integral on three time slots can then be merged into one time dependent factor. Furthermore, we obtain a second, time independent factor from the phase memory. Now, by using Eq. (26) one can see that the condition from Eq. (29) is fulfilled if

$$0 = 1 + \exp(ja_1) + \exp(ja_1) \exp(ja_2) \quad (30)$$

where  $a_r = 2\pi [\xi_m(3l+r) - \xi_{m'}(3l+r)]$  and we get  $-\exp(-ja_1) = 1 + \exp(ja_2)$ . By splitting this equation into imaginary and real parts, we have the following two conditions:

$$-1 = \cos(-a_1) + \cos(a_2) \quad (31)$$

$$0 = \sin(-a_1) + \sin(a_2). \quad (32)$$

This system has, modulo  $2\pi$ , two pairs of solutions

$$(a_1, a_2) \in \{(2\pi/3, 2\pi/3), (4\pi/3, 4\pi/3)\}. \quad (33)$$

Hence  $L^2$  orthogonality is achieved if  $\xi_m(3l+r) - \xi_{m'}(3l+r) = 1/3$  or  $\xi_m(3l+r) - \xi_{m'}(3l+r) = 2/3$  for  $r = 1, 2$  and for all combinations of  $m$  and  $m'$  with  $m \neq m'$ . In order to determine  $\xi_m(3l+r)$ , we detail in the following section the exact mapping and the correction factor.

### 2.2.2 Mapping

In this section we describe the mapping of the data sequence  $d_j$  to the data symbols  $d_{m,r}^{(l,1)}$  of the block code (Fig. 4). To obtain full rate each code block have to include three new symbols from the data sequence. In general, the mapping of the three new symbols has no restrictions. However, to fix a mapping two criteria are considered:

- mapping to simplify Eq. (29)
- low complexity of function  $\xi_m(3l+r)$ .



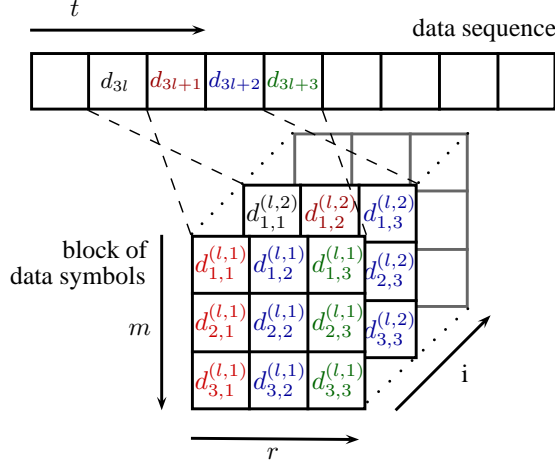


Figure 4: Mapping of the data sequence to the data symbols

The first criteria is already determined by using *parallel mapping* ( $d_{m,r}^{(l,i)} = d_{m',r}^{(l,i)}$ ). Therewith the mapping for the  $m$ -dimension (Fig. 4) is fixed. For the remaining two dimensions we choose a mapping similar to conventional CPM. The subsequent data symbols in  $r$ -direction are mapped to subsequent symbols from the data sequence. Also similar to conventional CPM we shift this mapping by  $-i$  and obtain

$$d_{m,r}^{(l,i)} = d_{3l+r-i+1}. \quad (34)$$

Eq. (35) and (36) show the simplification of the function  $\xi_m(3l+r)$ .

### 2.2.3 Correction Factor

The choice of the phase memory and therewith of the function  $\xi_m(3l+r)$  ensures the continuity of phase. If  $\phi_{m,r}((L_t l + r)T) = \phi_{m,r+1}((L_t l + r)T)$ , we always obtain the desired continuity. Hence,

$$\xi_m(L_t l + r) = h \sum_{i=1}^{\gamma} d_{m,r}^{(l,i)} q(iT) + c_{m,r}((3l+r)T) - h \sum_{i=1}^{\gamma} d_{m,r+1}^{(l,i)} q(iT) - c_{m,r+1}((3l+r)T). \quad (35)$$

With a mapping similar to conventional CPM (Section 2.2.2) we can simplify the two sums to a single term and obtain for  $r = 1, 2$

$$\xi_m(3l+r) = \frac{h}{2} d_{3l+r-\gamma+1} + c_{m,r}((3l+r)T) - c_{m,r+1}((3l+r)T). \quad (36)$$

As the data symbols are equal on each antenna, the difference between two different  $\xi_m(3l+r)$  does not depend on the data symbol  $d_{3l+r-\gamma+1}$ . Thus, when choosing *parallel mapping*,  $L^2$  orthogonality only depends on the correction factor.

To fulfill Eq. (30) for all antennas we take

- for  $m = 1, m' = 2$

$$a_r = \frac{2\pi}{3} = 2\pi[c_{1,r}((3l+r)T) - c_{1,r+1}((3l+r)T) - c_{2,r}((3l+r)T) + c_{2,r+1}((3l+r)T)], \quad (37)$$

- for  $m = 2, m' = 3$

$$a_r = \frac{2\pi}{3} = 2\pi[c_{2,r}((3l+r)T) - c_{2,r+1}((3l+r)T) - c_{3,r}((3l+r)T) + c_{3,r+1}((3l+r)T)] \quad (38)$$

- and for  $m = 1, m' = 3$  we consequently get

$$a_r = \frac{4\pi}{3} = 2\pi[c_{1,r}((3l+r)T) - c_{1,r+1}((3l+r)T) - c_{3,r}((3l+r)T) + c_{3,r+1}((3l+r)T)]. \quad (39)$$

The other three possible combinations of  $m$  and  $m'$  with  $m \neq m'$  lead only to a change of sign and we get  $a_r = -2\pi/3, -2\pi/3, -4\pi/3$ , respectively. Due to the modulo  $2\pi$  character of our condition, these are also valid solutions.

For simplicity, we assume similar correction factors for each time slot  $r$  of one Tx antenna  $c_{m,1}(t) = c_{m,2}(t) = c_{m,3}(t)$ . Since Eq. (39) arises from Eq. (37) and (38), we have two equations and three parameters:  $c_{1,r}(t)$ ,  $c_{2,r}(t)$  and  $c_{3,r}(t)$ . Hence we define  $c_{2,r}(t) = 0$  for  $r = 1, 2, 3$  and we get  $c_{1,r}((3l+r)T) - c_{1,r+1}((3l+r)T) = 1/3$  and  $c_{3,r}((3l+r)T) - c_{3,r+1}((3l+r)T) = -1/3$  for  $r = 1, 2$ . Codes fulfilling these conditions form the family of Parallel Codes (PC). We will now describe some possible solutions of this family.

An obvious solution for the correction factor is obtained for all functions which are 0 for  $t = (3l+r)T$  and  $\pm 1/3$  for  $t = (3l+r+1)T$ , e.g.

$$c_{1,r}(t) = -c_{3,r}(t) = \frac{2}{3} \cdot \frac{t - (3l+r)T}{2T} \quad (40)$$

for  $(3l+r)T \leq t \leq (3l+r+1)T$ . We denote this solution as linear parallel code (linPC). Of course, other choices are possible, e.g. based on raised cosine (rcPC).

Another way of defining the correction factor is

$$c_{1,r}(t) = -c_{3,r}(t) = \sum_{i=1}^{\gamma} \frac{2}{3} q(t - i'T) \quad (41)$$

for  $(3l+r)T \leq t \leq (3l+r+1)T$ . In that case we take advantage of the natural structure of CPM, i.e. in Eq. (35) all except one summands cancel down, similar to the terms with the data symbols. This definition has the advantage that we can merge the correction factor and the data symbol in Eq. (25) and we obtain two pseudo alphabets shifted by an offset (offPC) for the first and third transmitting antenna

$$\begin{aligned} \Omega_{d_1} &= \left\{ -M + 1 + \frac{2}{3h}, -M + 3 + \frac{2}{3h}, \dots, M - 1 + \frac{2}{3h} \right\} \\ \Omega_{d_3} &= \left\{ -M + 1 - \frac{2}{3h}, -M + 3 - \frac{2}{3h}, \dots, M - 1 - \frac{2}{3h} \right\}. \end{aligned}$$

Consequently, this  $L^2$ -orthogonal design may be seen as three conventional CPM signals with different alphabet sets  $\Omega_d$ ,  $\Omega_{d_1}$  and  $\Omega_{d_3}$  for each antenna. In this method, the constant phase offsets introduce frequency shifts. But as shown by the simulations in next section, these shifts are quite moderate.

## 2.3 Properties of PC CPM

### 2.3.1 Decoding

The optimal receiver for the proposed codes relies on the computation of a metric over complete ST blocks followed by a maximum-likelihood sequence estimation (MLSE).

Here, the metric is evaluated using the  $L^2$  norm

$$D_1 = \int_{3lT}^{(3l+3)T} \left| y_{1,r}(t) - \sum_{m=1}^3 \alpha_{1,m} s_{m,r}(t) \right|^2 dt. \quad (42)$$

For convenience, we use here only one receiving antenna but the extension to more than one is straightforward. The distance in Eq. (42) is obtained for all  $pM^{\gamma+L_t-1}$  possible variations of  $s_{m,r}(t)$  corresponding to the paths of the trellis.

The number of states can be reduced in two ways. First, by using the orthogonality property of the proposed code, all cross-correlations in Eq. (42) are canceled out and we obtain

$$D_2 = \sum_{m=0}^3 \sum_{r=0}^3 \int_{(3l+r)T}^{(3l+r+1)T} \left| y_{1,r}(t) - \alpha_{1,m} s_{m,r}(t) \right|^2 dt. \quad (43)$$

We only have to consider  $pM^\gamma$  paths for every  $s_{m,r}(t)$ . The complexity of computing the distance is therewith  $L_t^2 pM^\gamma$  which corresponds to the necessary effort to decode three symbols of three CPM signals.

Second, by taking advantage of the *parallel mapping* we are not forced to decode block-wise. We can compute the distances symbol-wise with

$$D_3 = \int_{\beta T}^{(\beta+1)T} \left| y_{1,r}(t) - \sum_{m=1}^3 \alpha_{1,m} s_{m,r}(t) \right|^2 dt \quad (44)$$

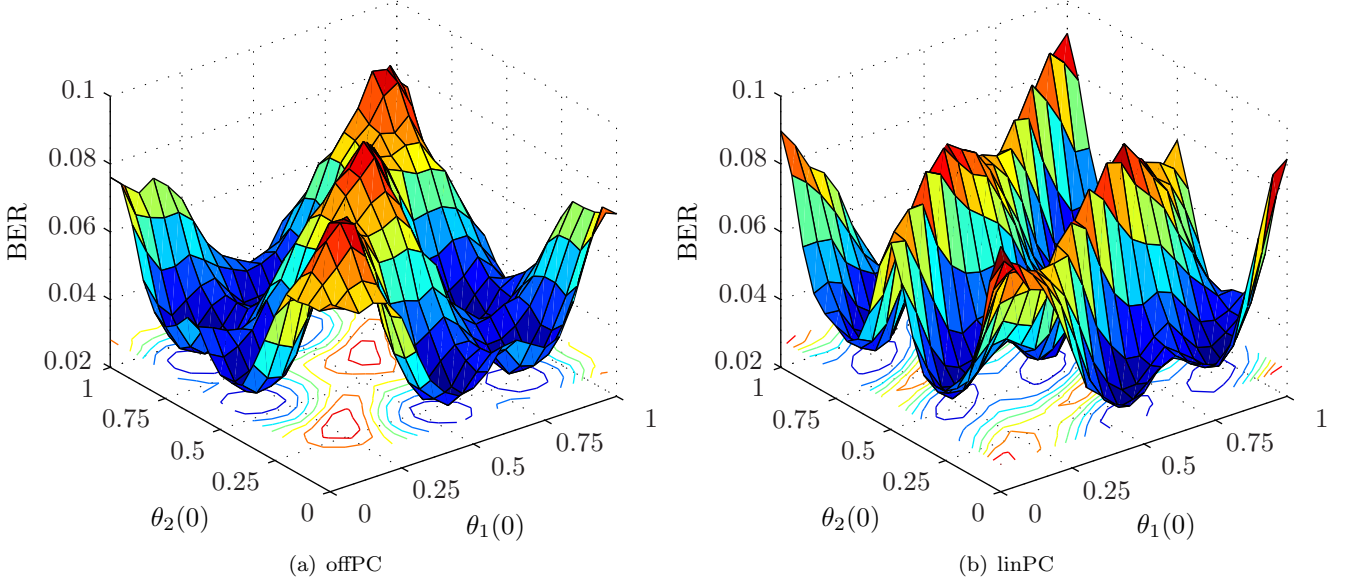


Figure 5: Simulation results for the BER with different initial phases  $\theta_i(0)$

with  $r = (\beta \bmod L_T) + 1$ . Similarly to conventional CPM,  $s_{m,r}(t)$  has  $pM^\gamma$  possible values which have to be evaluated for every antenna  $m$ . By doing that, we reduce the paths of the trellis but, at the same time, we increase the number of transitions in the trellis.

The number of paths can be further reduced by using some special properties of CPM. There exist numerous efficient algorithms for MLSE. However, the efficiency of the detection algorithm is not in the primary scope of this report and will be the subject of another upcoming paper.

### 2.3.2 Diversity

Simulations of the proposed code show a similar behavior as codes with full diversity. But, in contrast to  $L^2$  orthogonal code for two antennas [14], the diversity of the three antenna code depends on the initial phase  $\theta_i(0)$  of each antenna  $i$ . Figure 5 shows the simulation results for  $\theta_3(0) = 0$  and varying  $\theta_1(0)$  and  $\theta_2(0)$ . The bit error rate (BER) clearly depends on the choice of the initial phase. This effect is different for offset PC (Figure 5(a)) and linear PC (Figure 5(b)).

The shown simulation results are using 4-array CPM ( $M = 4$ ) at  $E_b/N_0 = 13dB$ . Further simulation with  $M = 8$  show no difference in the location of the minimal BER. Whereas the varying modulation indexes  $h$  slightly change the position of the minima.

## 2.4 Simulations

In this section we test the proposed algorithms by running MATLAB simulations. More precisely, we benchmark the offset parallel code (offPC) for two and three Tx antennas and the linear parallel code (linPC) for three Tx antennas. For all simulations we use a Gray-coded CPM with a modulation index of  $1/2$ , an alphabet of 2 bits per symbol ( $M = 4$ ) and a memory length  $\gamma$  of 2. We use a linear phase smoothing function  $q(t)$  (2REC). Corresponding to section 2.3.2, we use  $\theta_1(0) = 0.75$ ,  $\theta_2(0) = 15$  and  $\theta_3(0) = 0$  for linPC and  $\theta_1(0) = 0.45$ ,  $\theta_2(0) = 0.1$  and  $\theta_3(0) = 0$  for offPC.

The modulated signals are transmitted over a frequency flat Rayleigh fading channel with complex additive white Gaussian noise. The fading coefficients  $\alpha_{n,m}$  are constant for the duration of a code block (block fading) and known at the receiver (coherent detection). To guarantee a fair treatment of single and multi antenna systems the fading has to have a mean value of one.

The received signal  $y_n(t)$  is demodulated by the methods introduced in Section 2.3.1. Both require approximately the same computational effort and achieve the same performance. The evaluated distances are fed to the Viterbi algorithm (VA), which we use for MLSE. In these demodulation methods, the trellis which is decoded by the Viterbi algorithm has  $pM^{\gamma-1}$  states and  $M$  paths leaving each state. In our simulations, the Viterbi algorithm is truncated to a path memory of 10 code blocks, which means that we get a decoding delay of  $3 \cdot 10T$ .

Figure 6 shows the simulations results for one, two and three transmitting antennas. It can be seen that full diversity is probably achieved and that linPC and offPC perform equal well if the optimal initial phase is chosen.

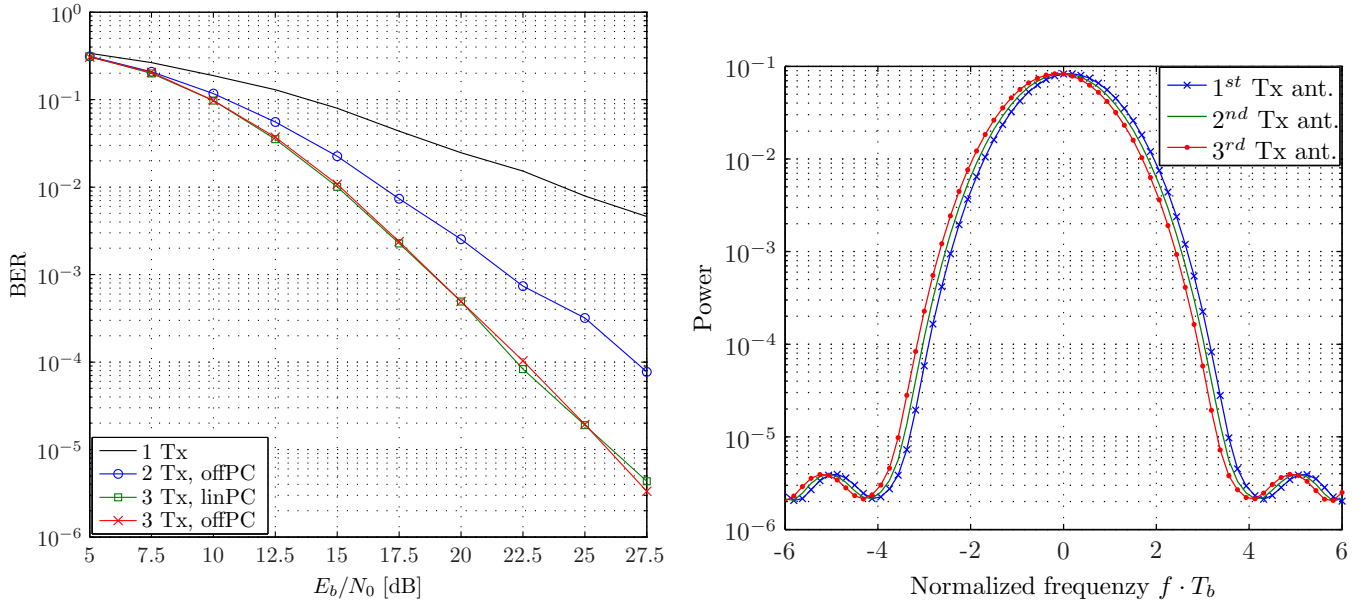


Figure 6: Left: Simulated bit error rate (BER) over a Rayleigh fading channel; Right: Power spectral density of the linPC analyzed with the Welch algorithm.

A main reason for using CPM for STC is the spectral efficiency. Figure 6 shows the simulated power spectral density (psd) obtained by the analysis of  $s_{m,r}(t)$  with the Welch algorithm. The psd of the offPC has a negligible difference compared to the linPC. Consequently it is not plotted in Figure 6. The second Tx antenna uses a conventional CPM signal without correction factor and hence shows an equal psd. The spectra of the other antennas are shifted due to the additional offset  $c_{mr}(t)$  with a non zero mean. Minimizing the  $L^1$ -norm of the difference between the unshifted and shifted spectra result in a phase difference of  $\pm 0.19$  measured in normalized frequency  $f \cdot T_d$ , where  $T_d = T/\log_2(M)$  is the bit symbol length. Compared to the frequency offset of 0.375 appearing for two  $L^2$ -orthogonal antennas, the three antenna system requires approximately the same bandwidth.

## 2.5 Conclusion to part two

In this part, we introduce a new family of  $L^2$ -orthogonal STC for three antennas. These systems are based on CPM supplemented by correction factors to ensure  $L^2$ -orthogonality. Structurally the proposed code family has full rate and we expect full diversity. Furthermore, we detail two simple representatives of the code family (offPC, linPC), where the offPC offers better performance and a very intuitive representation. By analyzing the power spectral density, it is also shown, that the extension of the bandwidth, caused by the correction factor, is small. Therefore the power efficiency of CPM is maintained.

## General conclusion

In this report, we detail the construction and analyze the properties of  $L^2$ -orthogonal STC-CPM for two and three transmitting antennas. These codes are attractive due to low-effort-decoding and the few restrictions the code-family set upon parameters of CPM. Also, the simulation results show the importance of optimizing the initial phases for an efficient design and an optimal use of parallel codes.

## References

- [1] X. Zhang and M. P. Fitz, "Space-time coding for Rayleigh fading channels in CPM system," *Proc. 38th Annu. Allerton Conf. Communication, Control, and Computing*, 2000.
- [2] D. Wang, G. Wang, and X.-G. Xia, "An orthogonal space-time coded partial response CPM system with fast decoding for two transmit antennas," *IEEE Trans. Wireless Commun.*, vol. 4, no. 5, pp. 2410 – 2422, 2005.
- [3] S. M. Alamouti, "A simple transmit diversity technique for wireless communications," *IEEE J. Sel. Areas Commun.*, vol. 16, no. 8, pp. 1451 – 1458, 1998.
- [4] V. Tarokh, H. Jafarkhani, and A. R. Calderbank, "Space-time block codes from orthogonal designs," *IEEE Trans. Inf. Theory*, vol. 45, no. 5, pp. 1456 – 1567, 1999.

- [5] X. Zhang and M. P. Fitz, "Space-time code design with continuous phase modulation," *IEEE J. Sel. Areas Commun.*, vol. 21, no. 5, pp. 783 – 792, 2003.
- [6] A. Zajić and G. Stüber, "A space-time code design for partial-response CPM: Diversity order and coding gain," *IEEE ICC*, 2007.
- [7] A.-M. Silvester, L. Lampe, and R. Schober, "Diagonal space-time code design for continuous-phase modulation," *GLOBECOM*, 2006.
- [8] G. Wang and X.-G. Xia, "An orthogonal space-time coded CPM system with fast decoding for two transmit antennas," *IEEE Trans. Inf. Theory*, vol. 50, no. 3, pp. 486 – 493, 2004.
- [9] J.B. Anderson, T. Aulin, and C.-E. Sundberg, *Digital Phase Modulation*, Plenum Press, 1986.
- [10] I. E. Telatar, "Capacity of multi-antenna gaussian channels," *European Trans. Telecommun.*, vol. 10, pp. 585 – 595, 1999.
- [11] G. J. Foschini and M. J. Gans, "On limits of wireless communications in a fading environment when using multiple antennas," *Wirel. Pers. Commun.*, vol. 6, no. 3, pp. 311–335, 1998.
- [12] V. Tarokh, N. Seshadri, and A. R. Calderbank, "Space-time codes for high data rate wireless communication: Performance criterion and code construction," *IEEE Trans. Inf. Theory*, vol. 44, no. 2, pp. 744 – 765, 1998.
- [13] G. Wang, W. Su, and X.-G. Xia, "Orthogonal-like space-time coded CPM system with fast decoding for three and four transmit antennas," *IEEE Globecom*, pp. 3321 – 3325, 2003.
- [14] M. Hesse, J. Lebrun, and L. Deneire, "L2 orthogonal space time code for continuous phase modulation," in *Proc. IEEE ICC*, *accepted for publication*, 2008.

